Microsc. Microanal. 21, 796–804, 2015
doi:10.1017/S1431927615014348

Microscopy AND Microanalysis

Simultaneous Observation of Cells and Nuclear Tracks from the Boron Neutron Capture Reaction by UV-C Sensitization of Polycarbonate

Agustina Portu,[1,2,*] Andrés Eugenio Rossini,[3] Silvia Inés Thorp,[4] Paula Curotto,[5] Emiliano César Cayetano Pozzi,[5] Pablo Granell,[6] Federico Golmar,[2,6,7] Rómulo Luis Cabrini,[1,8,9] and Gisela Saint Martin[1,10]

[1]*Department of Radiobiology, National Atomic Energy Commission (CNEA), Av. General Paz 1499, B1650KNA, San Martín, Buenos Aires, Argentina*
[2]*National Research Council (CONICET), Av. Rivadavia 1917, C1033AAJ, Ciudad Autónoma de Buenos Aires, Argentina*
[3]*Nuclear Regulatory Authority (ARN), Libertador 8250, C1429BNP, Ciudad Autónoma de Buenos Aires, Argentina*
[4]*Department of Instrumentation and Control, CNEA, Presbítero Juan González Aragón, B1802AYA, Ezeiza, Buenos Aires, Argentina*
[5]*Department of Research and Production Reactors, CNEA, Presbítero Juan González Aragón, B1802AYA, Ezeiza, Buenos Aires, Argentina*
[6]*Micro and Nanotechnology Centre of the Bicentennial (CNMB), National Institute of Industrial Technology (INTI), Av. Gral. Paz 5445, Ed. 42, B1650JKA, San Martín, Buenos Aires, Argentina*
[7]*School of Science & Technology, National University of San Martín (UNSAM), Martín de Irigoyen 3100, B1650JKA, San Martín, Buenos Aires, Argentina*
[8]*Faculty of Dentistry, University of Buenos Aires, Marcelo T. de Alvear 2142, C1122AAH, Ciudad Autónoma de Buenos Aires, Argentina*
[9]*Microspectrophotometry Laboratory (LANAIS-MEF), CONICET-CNEA, Av. General Paz 1499, B1650KNA, San Martín, Buenos Aires, Argentina*
[10]*Institute of Technology "Prof. Jorge Sabato", UNSAM, Av. General Paz 1499, B1650KNA, San Martín, Buenos Aires, Argentina*

Abstract: The distribution of boron in tissue samples coming from boron neutron capture therapy protocols can be determined through the analysis of its autoradiography image on a nuclear track detector. A more precise knowledge of boron atom location on the microscopic scale can be attained by the observation of nuclear tracks superimposed on the sample image on the detector. A method to produce an "imprint" of cells cultivated on a polycarbonate detector was developed, based on the photodegradation properties of UV-C radiation on this material. Optimal conditions to generate an appropriate monolayer of Mel-J cells incubated with boronophenylalanine were found. The best images of both cells and nuclear tracks were obtained for a neutron fluence of 10^{13} cm^{-2}, 6 h UV-C (254 nm) exposure, and 4 min etching time with a KOH solution. The imprint morphology was analyzed by both light and scanning electron microscopy. Similar samples, exposed to UV-A (360 nm) revealed no cellular imprinting. Etch pits were present only inside the cell imprints, indicating a preferential boron uptake (about threefold the incubation concentration). Comparative studies of boron absorption in different cell lines and *in vitro* evaluation of the effect of diverse boron compounds are feasible with this methodology.

Key words: neutron autoradiography, nuclear tracks, UV-C, BNCT, Mel-J, boron imaging, SEM, polycarbonate

Introduction

The distribution and localization of a particle emitter element in a sample can be determined through the autoradiography image produced on a solid state nuclear track detector (SSNTD) (Durrani & Bull, 1987). The use of these materials as heavy ion detectors is based on the fact that the damaged zones produced along the ion trajectories remain altered in a permanent way. These damaged zones or latent tracks can be amplified by a chemical attack (etching) with an appropriate solution. The etching velocity close to the ion trajectory is higher than the etching velocity in the bulk unirradiated material (V_b). This preferential attack velocity makes possible the development of the etch pits, or tracks, that can be observed by electron or optical microscopy, depending on the etching conditions (Fleischer et al., 1975).

SSNTD have been used for multiple applications since their first description by Young (1958), including radon and uranium dosimetry (e.g., Stegnar et al., 2013; Hadad et al., 2013), personal neutron dosimetry (e.g., Djeffal et al., 1997; Saint Martin et al., 2011), and detection of cosmic rays (e.g., Dey et al., 2011). One of the outstanding applications includes mapping heavy particle emitters in mineral and

Received December 15, 2014; accepted June 9, 2015
*Corresponding author. agustina.portu@gmail.com; portu@cnea.gov.ar

biological materials (e.g., Armijo and Rosenbaum 1967; Bersina et al., 1995; Thellier et al., 2001, Rodrigues et al., 2013; Chauhan & Chauhan, 2014). Indeed, the track density analysis on a detector put in contact with a tissue section that contains a heavy particle emitter allows determination of the spatial distribution of the element in the sample. This is the basis of autoradiographic analysis (Durrani & Bull, 1987).

Boron neutron capture therapy (BNCT) is a cancer treatment modality based on the selective accumulation of boron compounds in malignant tissue and the subsequent irradiation with thermal neutrons (e.g., Coderre et al., 2003). When the neutron capture reaction of ^{10}B takes place, α particles and ^{7}Li ions of high linear energy transfer and short path are emitted in opposite directions. Therefore, if most of the boron compound is accumulated in the cancer cells they are lethally damaged by these particles, preserving surrounding normal tissue. BNCT has been applied in different countries mostly for head and neck cancer, melanomas, and glioblastoma multiforme (e.g., Barth et al., 2012). The most commonly used compounds are boronophenylalanine (BPA) and sodium mercaptoundecahydro-closo-dodecaborate (GB-10), but there is active research searching for new more selective compounds (e.g., Tachikawa et al., 2014). The effectiveness of BNCT is mainly related to the selective accumulation of ^{10}B within cells, since the most relevant component of the total dose is given by the disintegration that follows the boron capture reaction.

Images formed by nuclear tracks in SSNTD have been extensively used to study the spatial distribution of boron for many years (e.g., Thellier et al., 1976; Larsson et al., 1984; Abe et al., 1986; Wittig et al., 2008). In our laboratory, the technique to obtain neutron autoradiographies of BNCT tissue samples in polycarbonate detectors was fully developed (Portu et al., 2011*a*, 2013). This method is being applied to qualitatively and quantitatively analyze boron distribution and concentration in different experimental models (e.g., Portu et al., 2011*b*; Molinari et al., 2015). The products of the $^{10}B(n,\alpha)$ ^{7}Li reaction originate the tracks on the polycarbonate. For that purpose the spatially correlated assembly of detector and tissue containing ^{10}B must be irradiated with thermal neutrons. Afterwards, the sample is detached from the detector, which is chemically etched to develop the latent tracks produced by the particles emitted from the tissue. Even though reference marks are usually applied (e.g., Portu et al., 2013; Tanaka et al., 2014), this procedure implies that the correlation between the emitter site and the corresponding track position can be determined with limited precision. Depending on the requirements of the application and the information expected to be obtained from the autoradiography, this limitation should be taken into account.

High resolution quantitative autoradiography (Solares & Zamenhof, 1995; Kiger et al., 2002) is a complex technique that allows simultaneous observation of tissue sections and nuclear tracks by using extremely thin SSNTD foils and a tissue protective system for preservation of the sample during chemical etching. Another method was proposed by Amemiya et al. (2002) to observe the sample image and nuclear tracks at the same time. It consists of producing an "engraved" replica of the biological sample on the detector foil surface that can be revealed by the same etching attack used to develop the nuclear tracks that originate in the boron atoms inside the sample. These authors obtained such images on CR39 (a commercial trademark for poly alyldiglicol carbonate, PADC) by irradiating the detector material with X rays and observation with an atomic force microscope. In later work the possibility of engraving the image of the biological sample on the CR39 detector with ultraviolet radiation was proposed, due to an increase in the bulk etching rate with UV exposure (Amemiya et al., 2005). The possibility of observing the obtained image with phase contrast optical microscopy was reported by Konishi et al. (2007).

In this work we studied the feasibility of obtaining a nuclear tracks image superimposed on the biological sample imprint in a polycarbonate (Lexan^{TM}) nuclear track detector. The goal was to establish optimal experimental conditions in order to set a simple observation method that allows simultaneous observation of the image corresponding to cells cultured on this detector and the tracks produced by the capture reaction in the boron atoms inside the cells. The most favorable cell culture conditions on a polycarbonate detector surface were found, ultraviolet radiation of two different wave lengths were checked, and best exposure time and etching conditions were determined. An *in vitro* melanoma experimental model was studied and a first assessment of the preferential boron uptake was made.

Materials and Methods

Cells

Cultures of Mel-J human melanoma cells established from pulmonary metastasis derived from a cutaneous malignancy were the biological model used to test the imprint generation (Guerra et al., 1989). Cells were seeded on 250 μm thick circular polycarbonate foils (Lexan™ 8010, SABIC Innovative Plastics, polished graphic grade), to be used as nuclear track detectors, which covered almost the entire bottom of 60 mm diameter Petri dishes. Polycarbonate foils were previously sterilized by embedding them in ethanol 70% for 4 h. During the 24 h previous to seeding, the foils were embedded in culture media. Cells were cultured in RPMI 1640 medium (Gibco) supplemented with antibiotics and 10% fetal bovine serum (Natocor) in a humid atmosphere with 5% CO_2 at 37°C. After 48 h (confluence of ≈60%,), cells were incubated in RPMI with BPA (10 μg ^{10}B/mL, Interpharma), for 2 h (Carpano et al., 2010). Then, the samples were washed three times with phosphate-buffered saline (PBS) and fixed in 2.5% glutaraldehyde (Biopack) at room temperature (in order to avoid cell shrinkage) for 15 min. Partial efflux of boron may occur during the fixation process, nevertheless intracellular motion is not a major concern for the actual application of the proposed technique.

Neutron Irradiation

The Lexan-fixed cells sets were irradiated at the BNCT facility of the RA-3 reactor (Ezeiza Atomic Center, Buenos Aires, Argentina) with a thermal neutron fluence of 10^{13} cm^{-2} to achieve the $^{10}B(n,\alpha)^{7}Li$ reaction. Neutron flux was previously measured using a Self Powered Neutron Detector (SPND), yielding an uncertainty of about 8% in the neutron fluence. During irradiation of the foils the flux was monitored at certain reference points to check its stability. Thermal neutron field characterization and dosimetry procedures are specified in Miller et al. (2009).

UV-C Irradiation

After neutron irradiation, three groups of samples were then irradiated with a 15 Watt, 254 nm wave length TUV G15T8 (Philips, Holland) lamp, for 2, 4 and 6 h, respectively. The irradiance had been previously measured at different distances from the lamp with a radiometer (International Light Technologies ILT77). At the irradiation position the irradiance was 4.65 ± 0.02 mW cm^{-2}. More details regarding the irradiation set up can be found in Portu et al. (2014).

UV-A Irradiation

Other samples were exposed to a 360 nm wavelength TLD 18 W/08 (Philips, Holland) lamp. Distance and time of exposure were set up in order to deliver the same energy/area (J cm^{-2}) received by the UV-C samples with the 6 h-exposure to UV-C.

Autoradiography

Samples were haematoxylin stained (BIOPUR), scanned and photographed with an Olympus DP70 microscope, equipped with a CCD camera. Reference points were taken into account in different zones in order to facilitate cell localization after the chemical attack of the detector foils. In this way a good correlation of a cell's images and their respective imprints was expected. Then the cells were removed from the detector surface with trypsin-EDTA (Sigma Life Science). Chemical etching of the Lexan foils was carried out with PEW solution (30 g KOH + 80 g ethyl alcohol + 90 g distilled water) at 70°C for different etching times (2, 3, and 4 min) for each UV-C irradiation group. New images, now of the cell's imprint, were obtained with the light microscope acquisition system.

Some foils that had been irradiated with UV-C or UV-A light were metallized with gold and observed in a scanning electron microscope (SEM) (FEI QUANTA 200). The height of the cell imprint was measured by a focused ion beam/SEM (FIB/SEM) dual beam system (Dual Beam FEI Helios Nanolab 650). First, a protective layer of Pt was deposited on top of the region of interest by ion beam induced deposition. Then, a cross section was milled with the ion beam to expose the inner part of the imprint at its center. The exposed cross section was then imaged by SEM and the height of the cell core was measured. The attacked thickness of UV-C irradiated material was measured with the same instrument.

Results and Discussion

In commercially available polystyrene Petri dishes used for routine cell culture, the polymer surface is treated by corona discharge and low pressure plasma to enhance the efficiency of cell adhesion (Amstein & Hartman, 1975; Curtis et al., 1983; Andrade, 1985). The material chosen as the nuclear track detector was polycarbonate, having shown several advantages over other SSTND in terms of boron quantification through nuclear track analysis (Portu et al., 2011*a*; Saint Martin et al., 2011). However, chemical inertness of the polymer surface hinders adhesion of cells, so numerous trials were necessary to find the conditions leading to good adhesion efficiency. Special care of certain parameters had to be taken: sudden temperature changes during cell seeding and washing were avoided, as well as modifications in pH when replacing the culture media. In Figure 1 the difference between a culture where cells are overlapped (a) and a monolayer of cells seeded on Lexan (b) can be observed. The individual thickness of one cell is, in many cases, shorter than the ranges of the fission reaction products. In cases where two or more cells were overlapped, the track density

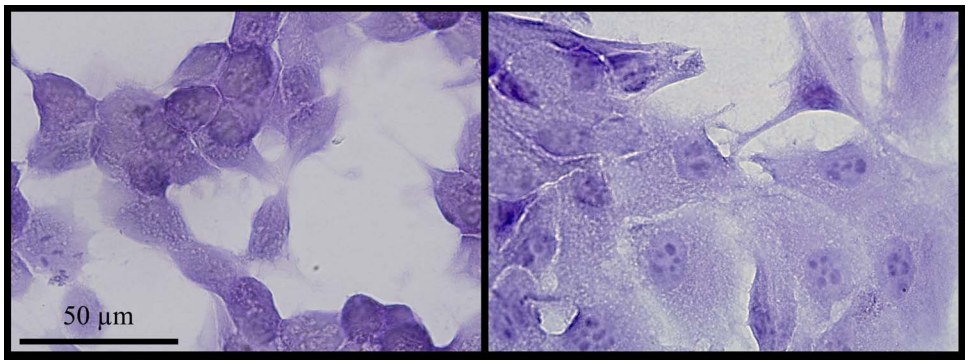

Figure 1. Haematoxylin stained Mel-J culture on Lexan. In the left panel, cells are superimposed, while in the right panel a monolayer was obtained.

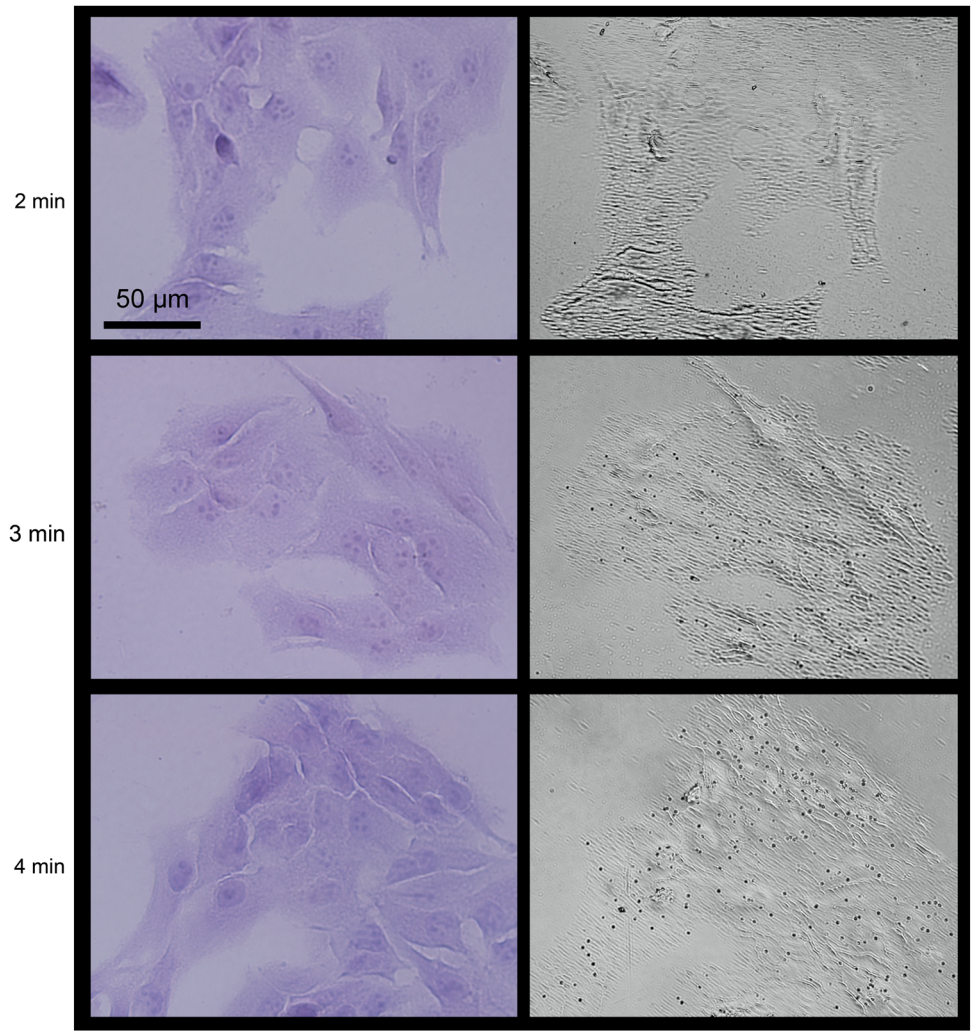

Figure 2. Mel-J cultures on Lexan and their corresponding autoradiography images. UV-C exposure: 2 h. Etching times with PEW solution (70°C): 2, 3, and 4 min.

quantified in that region would correspond to that cells' cluster. This fact leads to overestimation of the boron concentration per cell, so the existence of clusters of cells can prevent good assessment of intracellular boron content.

In Figures 2–4 examples of images corresponding to cells irradiated under different conditions and their respective imprints are shown. Polycarbonate sensitization due to UV-C light exposure is produced by photodegradation of the polymer and results in an imprint of biological material that faithfully reproduces the contours of cells and nuclei. From the analysis and comparison of samples processed in different conditions, optimal UV-C exposure times and chemical etching times were assessed.

Though cell imprints and track etch pits could be obtained for 2 h UV-C irradiation time, it was found that images of better quality could be achieved with longer UV-C exposure. Images corresponding to this UV irradiation condition are shown in Figure 2: cellular contours are somewhat diffuse regardless of the etching time. It was determined that an etching time of 2 min was insufficient because nuclear tracks were too small (diameter $\approx 1\,\mu$m) to be easily distinguished among the cell imprints.

In Figure 3 comparative images corresponding to 4 and 6 h UV-C exposure time and 3 and 4 min etching time are shown. The autoradiography images were taken focusing on the cellular imprint. Though nuclear tracks can be observed more clearly at another focal plane, they can still be seen as bright points. It can be noted that both cellular imprints and nuclear tracks exhibit slightly better features of definition and size at 6 h UV-C exposure time and 4 min etching time than for 4 h UV-C exposure and the same etching time. These were assumed to be the conditions leading to the best results for the imprint accomplishment.

It is worth mentioning that there are important differences between the technique proposed here and those presented in other works (Konishi et al., 2007), especially concerning the type of detector used and specific conditions of the involved procedures. Polycarbonate has advantageous threshold properties for the registration of particles coming from the BNC reaction, avoiding proton background that

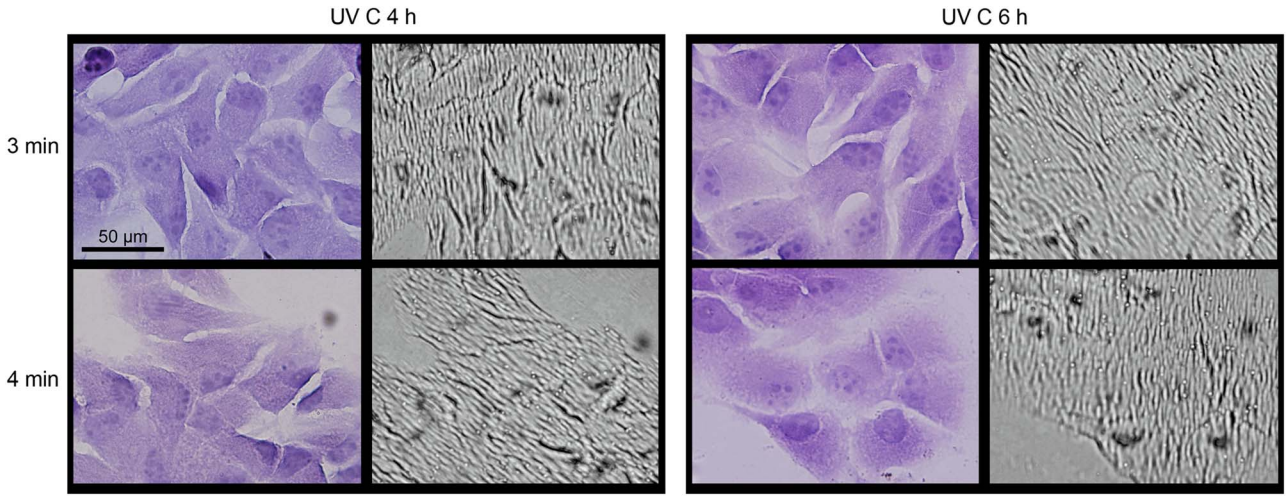

Figure 3. Mel-J cultures on Lexan and their corresponding autoradiography images. UV-C exposure: 4 h and 6 h. Etching times with PEW solution (70°C): 3 min and 4 min.

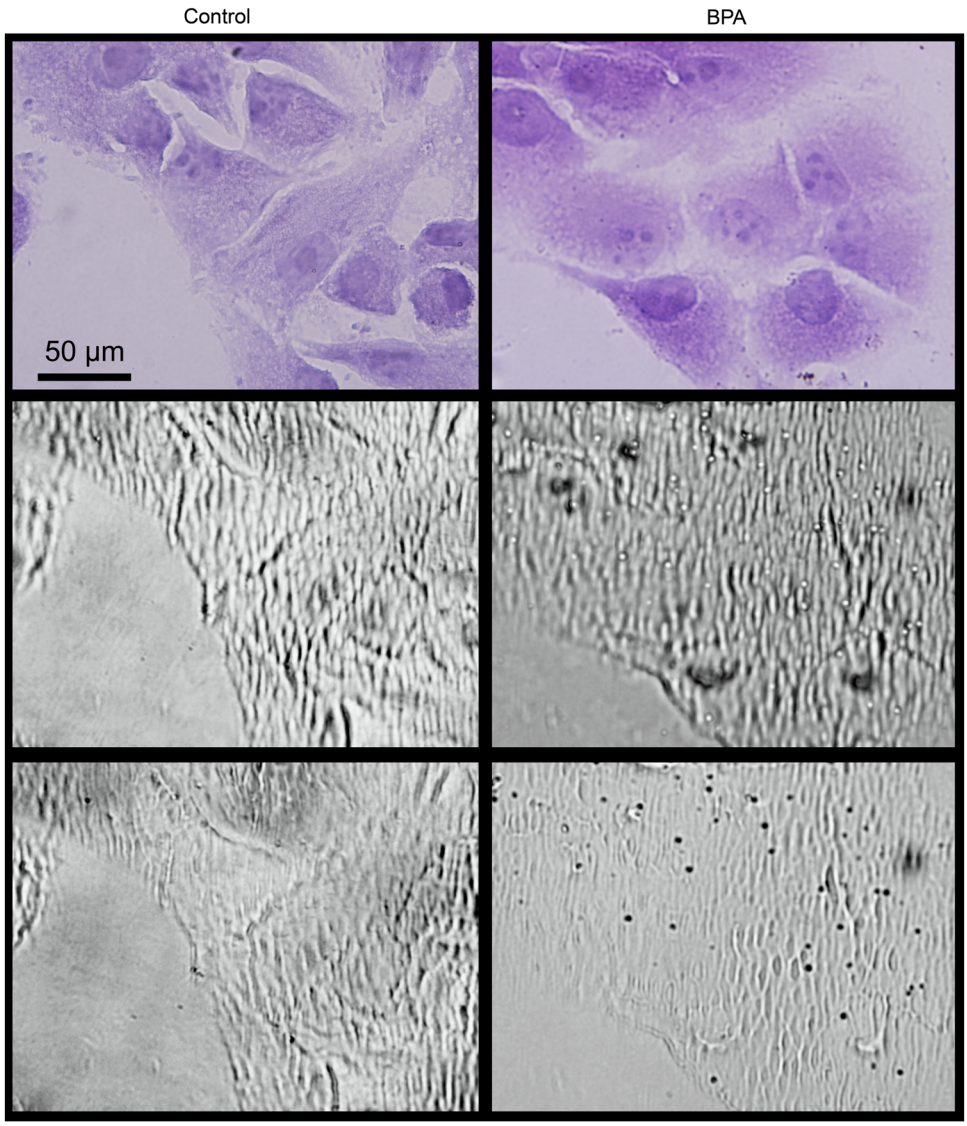

Figure 4. Mel-J cultures on Lexan and their corresponding autoradiography images, both control (left) and incubated with boronophenylalanine (right). UV-C exposure: 6 h. Etching times with PEW solution (70°C): 4 min.

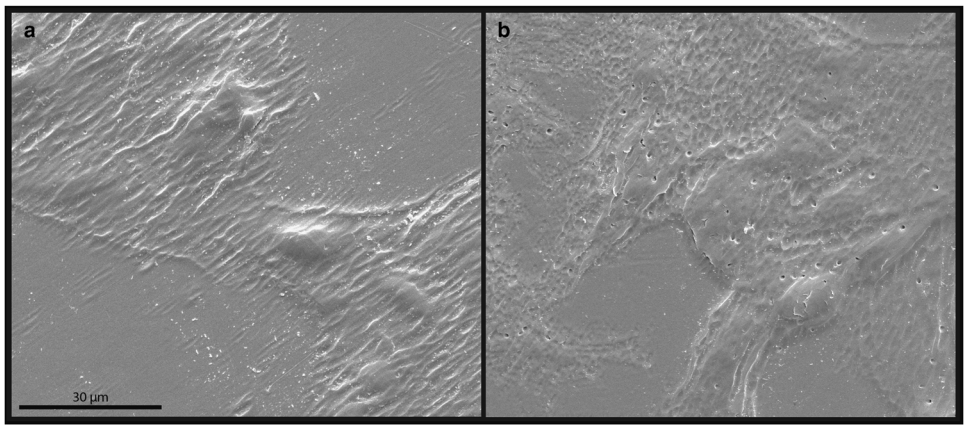

Figure 5. Scanning electron microscopy (SEM) images of cell imprints for (**a**) a control group and (**b**) incubated with boronophenylanaline.

originates in nitrogen atoms present in biological samples. On the other hand, adaptation of the technique for visualization of tracks and imprints in the bright field microscope, available in most laboratories, makes it possible to easily reproduce the set-up and extend it for other biological samples. Exploration and observation of samples with the light microscope is easy and faster than with more complex microscopy techniques, and the resulting images allow the analysis of boron distribution in cells.

In Figure 4 there are images of both control and BPA-samples, processed under optimal conditions. Nuclear tracks in control samples were completely absent, regardless of the UV-C exposure time or the etching duration. On the other hand they could be clearly observed in the autoradiographs corresponding to cells incubated with BPA. Images obtained for two different focal planes are shown: in the middle frame the cell imprint is in focus (nuclear tracks as bright circles), while in the lower frame the nuclear tracks are focused and can be seen as black circles.

SEM images confirmed that tracks appear as holes in the surface whereas the imprints can be seen as reliefs on the surface material (Fig. 5). Dark regions in the image correspond to depressions while bright areas are attributed to prominences, produced by cell nuclei. Cell relief is not uniform, and the measured maximum height is between 1.9 and 2.6 μm.

For all samples corresponding to BPA incubated cells, almost the totality of the nuclear tracks observed on the detector surface are concentrated in sites where cells had been placed. A concentration of 10 $\mu g\, g^{-1}$ of boron in the cell culture medium adopted in our study represents a value close to those determined in blood samples during clinical treatment (Fukuda et al., 1994). Furthermore, the 10 $\mu g\, g^{-1}$ value has been tested in previous studies of effectiveness of BNCT *in vitro* (Rossini et al., 2015).

In order to quantify track density, we first measured cell area by delimiting regions in the stained-culture image. In Figure 6a, a stairstep plot of the area per cell is shown. Afterwards, the track etch pits were counted in the previously delimited regions (mean value per cell: 16 ± 5). As the tracks were supposed to penetrate the detector with almost normal incidence, they were assumed to originate in

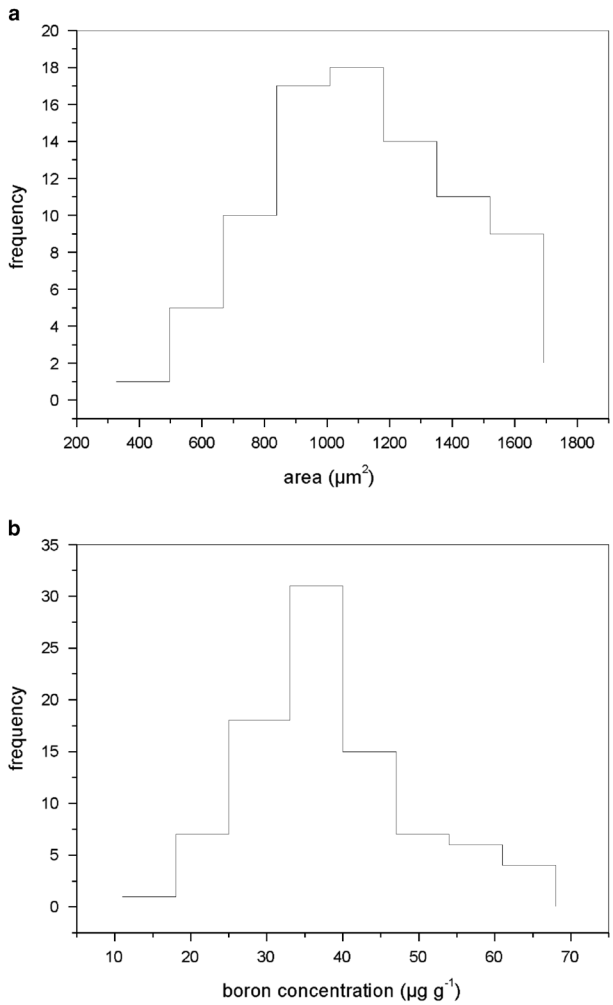

Figure 6. **a**: Cell area stairstep plot for a Mel-J culture. **b:** Boron concentration distribution per cell for a Mel-J culture incubated with boronophenylalanine (10 $\mu g\, g^{-1}$).

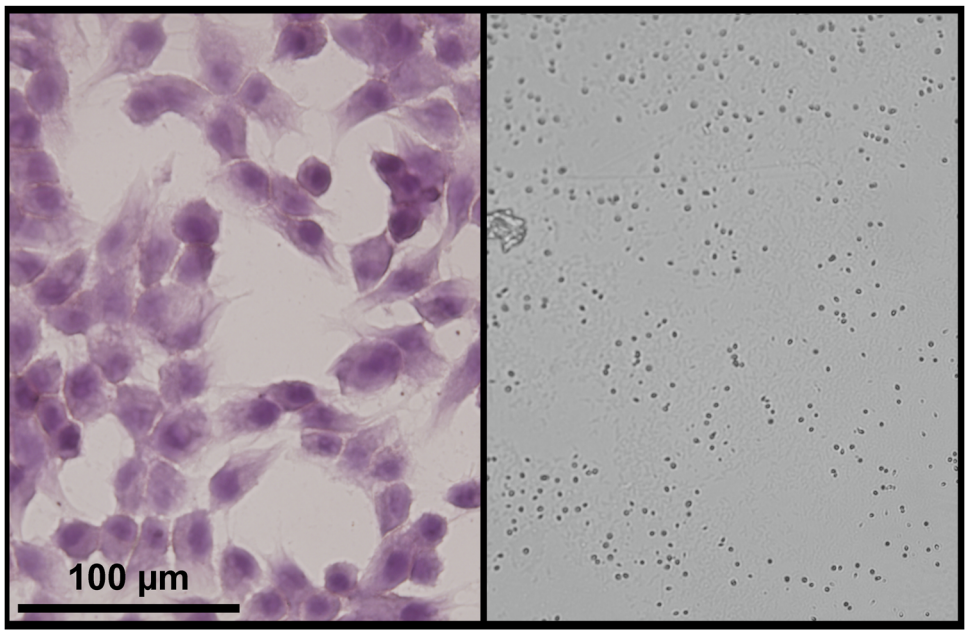

Figure 7. Mel-J culture on Lexan and its corresponding autorradiography image after UV-A exposure.

those delimited regions. By assuring a monolayer and avoiding cell clusters, we guaranteed that all the registered tracks came from only one cell per area of interest.

The track density value ($0.018 \pm 0.007\,\mu m^{-2}$) was interpolated in a calibration curve in order to obtain a boron concentration value. Calibration curves were established in previous work with aqueous boron enriched solutions irradiated in assemblies (Small Lexan Cases (SLCs)) developed for that purpose (Portu et al., 2011*a*). The standard foils were also exposed to UV-C radiation and chemically attacked at the optimal conditions. As can be observed in Figure 6b, not all the cells capture the same amount of boron: the mean value is $33 \pm 7\,\mu g\,g^{-1}$, which is about three times the originally incubated concentration. This result is in agreement with the activity of the neutral amino acid transporters (L), whose uptake efficacy is around 3–4 to 1 (Verrey, 2003; Rossini et al., 2015).

A system based on thinner standards than those actually used could be more adequate for quantification of boron in cell cultures. Thus, the evaluation of new reference materials that better resembles fixed cell samples is a matter of interest for future work. Moreover, it would also be worth studying variability in cell thickness as a possible source of uncertainty in the absolute quantification of boron using this technique.

In this work the possibility of obtaining an imprint of the biological sample with UV radiation of a different wavelength, that is, 360 nm (UV-A) was also studied. The irradiation conditions were chosen in order to compare with the case of 6 h exposure with UV-C. In Figures 7 and 8, nuclear tracks can be clearly observed, but no cell imprint is formed. From our results it could be concluded that the photo-induced damage mechanisms of the polymeric detector responsible for the imprint creation are more effective for photon energies higher than that corresponding

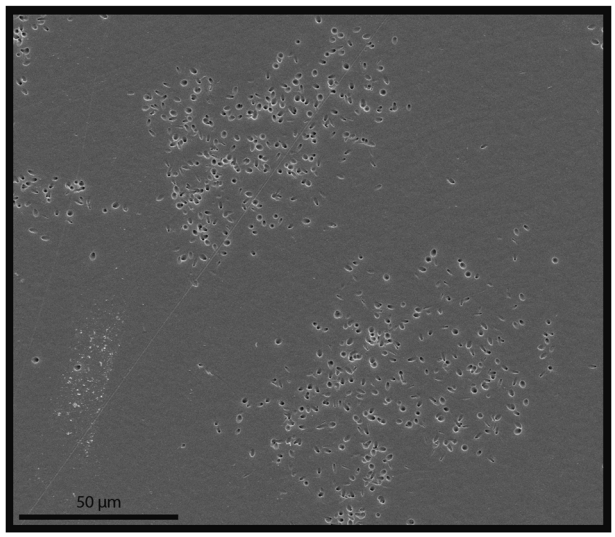

Figure 8. Scanning electron microscopy (SEM) image of tacks from a Mel-J culture incubated with boronophenylalanine, irradiated with UV-A.

to UV-A radiation. In fact, photo-induced reactions in polycarbonate have proven to be strongly dependant on wavelength (Andrady et al., 1991; Rivaton, 1995). Photodegradation of polycarbonate is a surface reaction, evidenced by the material yellowing. It is a very complex process and a variety of competing mechanisms are proposed to explain it (Diepens & Gijsman, 2007). Main chain scission in polycarbonate was found to take place more efficiently with 260 nm light (Torikai et al., 1993). As chemical attack velocity in the damaged detector material is related to molecular weight and chain fragment length, the feasibility of revealing the cell imprint could be ascribed to preferential etching

velocities in the UV-C irradiated samples. Indeed, increase in the V_b of UV-C irradiated material was $30.2 \pm 0.6\ \mu m\ h^{-1}$, resulting in a V_b more than twice the V_b corresponding to non-irradiated material ($19.2 \pm 0.6\ \mu m\ h^{-1}$).

This technique could make significant contributions as a tool for assessing boron concentration *in vitro*. As a first approach this knowledge can be useful for understanding the patterns of energy deposition in BNCT.

Conclusions

A method is proposed that allows simultaneous display of nuclear tracks originating at ^{10}B atoms inside Mel-J cells grown on Lexan polycarbonate nuclear track detector, improving spatial resolution of the autoradiography technique applied to cell cultures. The use of light microscopy for the exploration and observation of samples simplifies and accelerates the application of the technique. Optimal cell culture conditions leading to good adhesion efficiency and monolayer cell disposition were attained.

It could be observed that UV exposure of higher wave length (360 nm) was not effective to produce cell imprints on the polycarbonate detector. Best UV-C light irradiation and etching time conditions were established in order to obtain the more accurate imprint of the cells, as well as the tracks corresponding to Li ions and alpha particles that originated in the ^{10}B neutron capture reaction. With this procedure it is possible to estimate the incorporation of ^{10}B in different physiological situations at the cellular level. Consequently, it is possible to evaluate boron uptake capacity of the cell line under study. An immediate application of this method is the assessment of events per cell in different cell lines.

Acknowledgments

This study was partially supported by a grant from the Florencio Fiorini Foundation. The authors are grateful to Adriana Dominguez of the Electronic Microscopy Group (Department of Materials, CNEA) for technical assistance.

References

Abe, M., Amano, K., Kitamura, K., Tateishi, J. & Hatanaka, H. (1986). Boron distribution analysis by alpha-autoradiography. *J Nucl Med* **27**, 677–684.

Amemiya, K., Takahashi, H., Nakazawa, M., Shimizu, H., Majima, T., Nakagawa, Y., Yasuda, N., Yamamoto, M., Kageji, T., Nakaichi, M., Hasegawa, T., Kobayashi, T., Sakurai, Y. & Ogura, K. (2002). Soft X-ray imaging using CR-39 plastics with AFM readout. *Nucl Instr Meth B* **187**, 361–366.

Amemiya, K., Takahashi, H., Kajimoto, Y., Nakazawa, M., Yanagie, H., Hisa, T., Eriguchi, M., Nakagawa, Y., Majima, T., Kageji, T., Sakurai, Y., Kobayashi, T., Konishi, T., Hieda, K., Yasuda, N. & Ogura, K. (2005). High-resolution nuclear track mapping in detailed cellular histology using CR-39 with the contact microscopy technique. *Radiat Meas* **40**, 283–288.

Amstein, C.F. & Hartman, P.A. (1975). Adaption of plastic surfaces for tissue culture by glow discharge. *J Clin Micrbiol* **2**, 46–54.

Andrade, J.D. (1985). *Surface and Interfacial Aspects of Biomedical Polymers*. New York, USA: Plenum Press.

Andrady, A.I., Fueki, K. & Torikai, A. (1991). Spectral sensitivity of polycarbonate to light-induced yellowing. *J Appl Polym Sci* **42**, 2105–2107.

Armijo, J.S. & Rosenbaum, H.S. (1967). Boron detection in metals by alpha-particle tracking. *J Appl Phys* **38**, 2064–2069.

Barth, R.F., Vicente, M.G., Harling, O.K., Kiger, W.S. III, Riley, K.J., Binns, P.J., Wagner, F.M., Suzuki, M., Aihara, T., Kato, I. & Kawabata, S. (2012). Current status of boron neutron capture therapy of high grade gliomas and recurrent head and neck cancer. *Radiat Oncol* **7**, 146.

Bersina, I.G., Brandt, R., Vater, P., Hinket, K. & Schütze, M. (1995). Fission track autoradiography as a means to investigate plants for their contamination with natural and technogenic uranium. *Rad Meas* **24**, 271–282.

Carpano, M., Dagrosa, A., Nievas, S., Rossini, A., Juvenal, G. & Pisarev, M. (2010). Comparative studies of boronophenylalanine (BPA) uptake in three human cell lines of malignant melanoma. In *Proceedings of 14th International Congress on Neutron Capture Therapy*, Comisión Nacional de Energía Atómica (ed.), pp. 123–125. Argentina: Comisión Nacional de Energía Atómica.

Chauhan, P. & Chauhan, R.P. (2014). Variation in alpha radioactivity of plants with the use of different fertilizers and radón measurement in fertilized soil samples. *J Environ Health Eng* **12**, 1–8.

Coderre, J.A., Turcotte, J.C., Riley, K.J., Binns, P.J., Harling, O.K. & Kiger, W.S. (2003). Boron neutron capture therapy: Cellular targeting of high linear energy transfer radiation. *Technol Cancer Res Treat* **2**, 355–375.

Curtis, A.S.G., Forrester, J.V., Mcinnes, C. & Lawrie, F. (1983). Adhesion of cells to polystyrene surfaces. *J Cell Biology* **97**, 1500–1506.

Dey, S., Gupta, D., Maulik, A., Raha, S., Saha, S.K., Syam, D., Pakarinen, J., Voulot, D. & WENANDER, F. (2011). Calibration of a solid state nuclear track detector (SSNTD) with high detection threshold to search for rare events in cosmic rays. *Astropart Phys* **34**, 805–808.

Diepens, M. & Gijsman, P. (2007). Photodegradation of bisphenol-A polycarbonate. *Polym Degrad Stab* **92**, 397–406.

Djeffal, S., Lounis, Z., Allab, M. & Izerrouken, M. (1997). Further investigations on CR-39 fast neutron personal dosemeter. *Nucl Instr Meth Phys A* **98**, 343–350.

Durrani, S.A. & Bull, R.K. (1987). Further applications of track detectors and some directions for the future. *Solid State Nuclear Track Detection. Principles, Methods and Applications.* International Series in Natural Philosophy, Oxford, UK: Pergamon Press, pp. 250–253.

Fleischer, R.L., Price, P. & Walker, R.M. (1975). *Nuclear Tracks in Solids*. Berkeley, USA: University of California Press.

Fukuda, H., Hiratsuka, J., Honda, C., Kobayashi, T., Yoshino, K., Karashima, H., Takahashi, J., Abe, Y., Kanda, K., Ichihashi, M. & Mishima, Y. (1994). Boron neutron capture therapy of malignant melanoma using ^{10}B-paraboronophenylalanine with special reference to evaluation of radiation dose and damage to the normal skin. *Radiat Res* **138**, 435–442.

Guerra, L., Mordoh, J., Slavutsky, I., Larripa, I. & Medrano, E.E. (1989). Characterization of IIB-MEL-J: A new and highly heterogenous human melanoma cell line. *Pigment Cell Res* **2**, 504–509.

Hadad, K., Sarshough, S., Faghihi, R. & Taheri, M. (2013). Application of polystyrene films for indoor radon dosimetry as SSNTD. *Appl Radiat Isot* **74**, 23–25.

Kiger, W.S. 3RD, Micca, P.L., Morris, G.M. & Coderre, J.A. (2002). Boron microquantification in oral muscosa and skin following administration of a neutron capture therapy agent. *Radiat Prot Dosimetry* **99**, 409–412.

Konishi, T., Amemiya, K., Natsume, T., Takeyasu, A., Yasuda, N., Furusawa, Y. & Hieda, K. (2007). A new method for the simultaneous detection of mammalian cells and ion tracks on a surface of CR 39. *J Radiat Res* **48**, 255–261.

Larsson, B., Gabel, D. & Borner, H.G. (1984). Boron-loaded macromolecules in experimental physiology: Tracing by neutron capture radiography. *Phys Med Biol* **29**, 361–370.

Miller, M., Quintana, J., Ojeda, J., Langan, S., Thorp, S., Pozzi, E., Sztejnberg, M., Estryk, G., Nosal, R., Saire, E., Agrazar, H. & Graiño, F. (2009). New irradiation facility for biomedical applications at the RA-3 reactor thermal column. *Appl Radiat Isot* **67**, 226–229.

Molinari, A.J., Thorp, S.I., Portu, A.M., Saint Martin, G., Pozzi, E.C., Heber, E.M., Bortolussi, S., Itoiz, M.E., Aromando, R.F., Monti Hughes, A., Garabalino, M.A., Altieri, S., Trivillin, V.A. & Schwint, A.E. (2015). Assessing advantages of sequential boron neutron capture therapy (BNCT) in an oral cancer model with normalized blood vessels. *Acta Oncol* **54**, 99–106.

Portu, A., Bernaola, O.A., Nievas, S., Liberman, S. & Saint Martin, G. (2011*a*). Measurement of ^{10}B concentration through autoradiography images in polycarbonate nuclear track detectors. *Rad Meas* **46**, 1154–1159.

Portu, A., Carpano, M., Dagrosa, A., Nievas, S., Pozzi, E., Thorp, S., Cabrini, R., Liberman, S. & Saint Martin, G. (2011*b*). Reference systems for the determination of ^{10}B through autoradiography images: Application to a melanoma experimental model. *Appl Radiat Isot* **69**, 1698–1701.

Portu, A., Carpano, M., Dagrosa, A., Cabrini, R. & Saint Martin, G. (2013). Qualitative autoradiography with polycarbonate foils enables histological and track analyses on the same section. *Biotech Histochem* **88**, 217–221.

Portu, A., Rossini, A., Gadan, M.A., Bernaola, O.A., Thorp, S.I., Curotto, P., Pozzi, E.C.C., Cabrini, R.L. & Saint Martin, G. (2014). Experimental set up for the irradiation of biological samples and nuclear track detectors with UV C. *RPOR*, Ahead of print, http://dx.doi.org/10.1016/j.rpor.2014.10.003.

Rivaton, A. (1995). Recent advances in bisphenol-A polycarbonate photodegradation. *Polym Degrad Stab* **49**, 163–179.

Rodrigues, G., Arruda-Neto, J.D.T., Pereira, R.M.R., Kleeb, S.R., Geraldo, L.P., Primi, M.C., Takayama, L., Rodrigues, T.E., Cavalcante, G.T., Genofre, G.C., Semmler, R., Nogueira, G.P. & Fontes, E.M. (2013). Uranium deposition in bones of Wistar rats associated with skeleton development. *Appl Radiat Isot* **82**, 105–110.

Rossini, A., Dagrosa, M.A., Portu, A., Saint Martin, G., Thorp, S., Casal, M., Navarro, A., Juvenal, G.J. & Pisarev, M.A. (2015). Assessment of biological effectiveness of boron neutron capture therapy in primary and metastatic melanoma cell lines. *Int J Radiat Biol* **91**, 81–89.

Saint Martin, G., Portu, A., Santa Cruz, G.A. & Bernaola, O.A. (2011). Stochastic simulation of track density in nuclear track detectors for ^{10}B measurements in autoradiography. *Nucl Instr Meth Phys B* **269**, 2781–2785.

Solares, G.R. & Zamenhof, R.G. (1995). A novel approach to the microdosimetry of neutron capture therapy. Part I. High resolution quantitative autoradiography applied to microdosimetry in neutron capture therapy. *Radiat Res* **144**, 50–58.

Stegnar, P., Shishkov, I., Burkitbayev, M., Tolongutov, B., Yunusov, M., Radyuk, R. & Salbu, B. (2013). Assessment of the radiological impact of gamma and radon dose rates at former U mining sites in Central Asia. *J Environ Radiact* **123**, 3–13.

Tanaka, H., Sakurai, Y., Suzuki, M., Masunaga, S.I., Takamiya, K., Maruhashi, A. & Ono, K. (2014). Development of a simple and rapid method of precisely identifying the position of ^{10}B atoms in tissue: An improvement in standard alpha autoradiography. *J Radiat Res* **55**, 373–380.

Tachikawa, S., Miyoshi, T., Koganei, H., El-Zaria, M.E., Viñas, C., Suzuki, M., Ono, K. & Nakamura, H. (2014). Spermidinium closo-dodecaborate-encapsulating liposomes as efficient boron delivery vehicles for neutron capture therapy. *Chem Commun* **50**, 12325–12328.

Thellier, T., Stelz, T. & Wissocq, J.C. (1976). Detection of stable isotopes of lithium or boron with the help of A (n,alpha) nuclear reaction. Application to the use of ^{6}Li as a tracer for unidirectional flux measurements and to the microlocalization of lithium in animal histologic preparations. *Biochim Biophys Acta* **43**, 604–627.

Thellier, M., Dérue, C., Tafforeau, M., Le Sceller, L., Verdus, M.C., Massiot, P. & Ripoll, C. (2001). Physical methods for in vitro analytical imaging in the microscopic range in biology, using radioactive or stable isotopes (review article). *J Trace Microprobe T* **19**, 143–162.

Torikai, A., Mitsuoka, T. & Fueki, K. (1993). Wavelength sensitivity of the photoinduced reaction in polycarbonate. *J Polym Sci Part A: Polym Chem* **31**, 2785–2788.

Verrey, F. (2003). System L: Heteromeric exchangers of large, neutral amino acids involved in directional transport. *Eur J Physiol* **445**, 529–533.

Wittig, A., Michel, J., Moss, R.L., Stecher-Rasmussen, F., Arlinghaus, H.F., Bendel, P., Mauri, P.L., Altieri, S., Hilger, R., Salvadori, P.A., Menichetti, L., Zamenhof, R. & Sauerwein, W.A. (2008). Boron analysis and boron imaging in biological materials for boron neutron capture therapy (BNCT). *Crit Rev Oncol Hematol* **68**, 66–90.

Young, D.A. (1958). Etching of radiation damage in lithium fluoride. *Nature* **182**, 357–377.